In: Trends in Copepod Studies - Distribution, Biology and Ecology ISBN 0000000000
Editor: Marco Uttieri, pp. 1-14

Chapter 1

CHEMOSENSATION AND POTENTIAL NEURONAL MECHANISM OF RATIO DETECTION IN A COPEPOD

William Langhoff [*] Peter Hinow[*†] J. Rudi Strickler[‡§] Jeannette Yen[¶]

July 11, 2017

Abstract

Male copepods of the species *Temora longicornis* are able to follow a pheromone trail laid out by a female. Moreover, the male is able to change the direction of its movement if it initially follows the trail in the wrong direction. Previously, we proposed that the female pheromone may be blend of multiple compounds with different chemical properties and that the male senses their ratio rather than an absolute concentration. This allows for a better method to decide in which direction to move. Here we implement a simple, yet efficient design for the olfactory apparatus using the Leaky Integrate-and-Fire neuronal model. We implement a Simulated Annealing algorithm for the selection of optimal synaptic weights and show that the circuit enables ratio detection over a wide array of input signals. Our results encourage further research on similarities of brain organization in copepods and airborne arthropods in which ratio detection plays an important role.

1. Introduction

At a population density of about one individual per liter of water in the world ocean, copepods are the most abundant class and the greatest reservoir of organic carbon among all

[*]Department of Mathematical Sciences, University of Wisconsin - Milwaukee, Milwaukee, WI, USA
[†]Corresponding author. Email: hinow@uwm.edu
[‡]Department of Biological Sciences, University of Wisconsin - Milwaukee, Milwaukee, WI, USA
[§]Marine Science Institute, University of Texas, Port Aransas, TX, USA
[¶]School of Biological Sciences, Georgia Institute of Technology, Atlanta, GA, USA

In: Trends in Copepod Studies - Distribution, Biology and Ecology ISBN 0000000000
Editor: Marco Uttieri, pp. 2-14

animals. They constitute a key link between autotrophic phytoplankton and higher trophic levels in freshwater and marine food webs. Thus their ecology has tremendous implications on other life forms, all the way to land and air based animals. Current challenges to their well-being include anthropogenic acidification and chemical pollution of their natural habitats. It is imperative to understand their ecology, in particular their mating behavior, to predict whether and how these challenges may be met by the world's copepods.

Copepods are sexual animals and their mating behavior has been a fascinating research topic for two centuries. Katona (1973) proposed that copepods use chemical signaling mechanisms to find each other in the dark and three-dimensional water column. This view was substantiated in a series of works at the turn of the 21st century (Bagøien and Kiørboe, 2005; Doall *et al.*, 1998; Seuront, 2013; Weissburg *et al.*, 1998; Tsuda and Miller, 1998; Yen *et al.*, 2004). Males often display swimming adaptations aimed at increasing the encounter success with conspecific females (Nihongi *et al.*, 2004; Uttieri *et al.*, 2007; Yen and Lasley, 2011). A key observation by Doall *et al.* (1998) was that when a male *Temora longicornis* finds the trail laid by a female, but begins the pursuit in the wrong direction, he is able to turn around and to continue until he has reached the female. This happens within a remarkably short time, after only 1-2 *s* of pursuit in the wrong direction (Figure 1). The observations of Doall *et al.* (1998) do not indicate that the males know the direction of the female at the moment of finding the trail.

In earlier work (Hinow *et al.*, 2017) we presented a simple mathematical description of how the directional information can be encoded in the pheromone trail left behind by the female. Even in quiet and undisturbed water, any compound emitted by the female is subject to diffusion and chemical decay reactions. In the fixed frame of the moving female, the concentrations of the compound(s) form an idealized one-dimensional trail of concentrations that decrease with the distance from the female. A searching agent (the male) can be equipped in one of two ways. On the one hand, it can attempt to detect a change in the absolute concentration of a single compound. If the concentration is increasing in the direction of the motion, it should continue in that direction; if the concentration is decreasing in the direction of the motion, it should turn around. On the other hand, the female can emit two compounds at roughly the same rate that differ however in their decay or diffusion rates. At a distance from the female, the male will encounter these compounds in a ratio that differs from 1. The direction of the motion should be maintained if the ratio approaches 1 and it should be reversed otherwise. Using mathematical modeling and simulation we found evidence that an agent able to detect a ratio outperforms an agent that is dependent on the gradient of a single compound (Hinow *et al.*, 2017). Indeed, if the initial direction of motion is opposite to the direction of the moving female, it is possible to enter the trail further away from the female and still make the turn. Moreover, the threshold in the signal change required for turning can be chosen bigger.

Extracting directional information from chemical cues is an important task for a large number of animal species though the precise mechanisms often remain only partially understood. A well-known example are dogs *(Canis familiaris)* with special breeds for tracking purposes (Wells and Hepper, 2003; Hepper and Wells, 2005; Gadbois and Reeve, 2014). Ratio detection of chemicals has been investigated in a number of species (Clifford and Riffell, 2013; Wyatt, 2010), most notably in moths and other lepidopterans (Belmabrouk *et al.*, 2011; deBruyne and Baker, 2008; Zavada *et al.*, 2011). In various moth species

In: Trends in Copepod Studies - Distribution, Biology and Ecology ISBN 0000000000
Editor: Marco Uttieri, pp. 3-14

where the chemical components of the pheromone blends have been identified, sympatric sister species use identical components of the mixture, albeit in different ratios. Zavada *et al.* (2011) proposed a simple competition-based neuronal model that is capable to compare the strengths of two signals and to lead a search towards a region where the signals are in the desired ratio. Their model is composed of sets of Olfactory Receptor Neurons (ORNs) that excite Local Neurons (LNs) of different types. The local neurons, in turn, are connected by inhibitory synapses. The presence of multiple compounds in the moth pheromone blend indicates that species-specific information is also conveyed. This can help to maintain species integrity, provided that the ratios of the components remain stable in the plume. Hinow *et al.* (2017) postulated that the ratio of components needs to change over time so that the trail can point toward the animal that laid it.

The goal of this chapter is to revisit the observations of Doall *et al.* (1998) in light of newer insights gained from chemically modulated mating behavior in airborne insects. We begin by reviewing in part the Schlieren optical technique pioneered by Töpler (1866) and its application to the capture of small translucent animals in water in Section 2. In Section 3 we consider a simplified version of the neuronal model proposed in Zavada *et al.* (2011). Instead of modeling the neurons by sophisticated models such as the one by Hodgkin and Huxley (1952), we use the Leaky Integrate-and-Fire (LIF) model (Gerstner *et al.*, 2014). This model can be traced back to Louis Lapicque (1907) from a time long before mechanisms generating neuronal action potentials were known (Abbott, 1999; Brunel and van Rossum, 2007). The LIF model is widely used today. Its main advantage, the computational simplicity, allows a focus on questions of design of circuitry. In Section 4 we implement the Simulated Annealing (SA) (Press *et al.*, 2007) algorithm to optimize the synaptic weights of the network. We find that a simple network model consisting of LIF neurons with conductance-based synaptic weights can implement a ratio detection mechanism. The optimal synaptic weights for the model indicate a strong mutual inhibition of the specialist and generalist local neurons. The relative simplicity of the network topology lends credibility to the thesis that ratio detection evolved early on in the ancestry of today's marine copepods.

2. Observations of *Temora longicornis*

Most if not all photographs taken by the public at large are of "amplitude objects". In such an object, spatial differences in color values make it visible on the image. To image a clear wine glass submerged in clear water is one of the biggest challenges in photography. Special lighting at special angles may reflect from the surfaces to show parts of the glass. What has not been used in this case is the fact that the glass has a different refractive index than water. In such an environment, the glass should be looked at as a "phase object", and the optical techniques of making phase objects visible would render a distinct image of the glass. Phase objects with their refractive index slow down the light, creating a difference between light passing through the object and light from the background. Schlieren and shadowgraph techniques (Settles, 2001) render images based on differences in refractive indices. To employ these optical techniques became easier with the advent of single-line lasers and optics that allow collimated light beams carrying the information of an object for a long distance. For example, in our case, copepods swimming in a 1.5 L volume of

In: Trends in Copepod Studies - Distribution, Biology and Ecology ISBN 0000000000
Editor: Marco Uttieri, pp. 4-14

water ($10 \times 10 \times 15$ cm) were imaged by a camera 2.16 m away with a resolution of 0.1 mm (Strickler, 1977, 1998; Doall *et al.*, 1998; Strickler and Hwang, 1999).

Using collimated laser beams emitting laser light at one wavelength adds another component that can be used to observe particles of different sizes in 3D and suspended in volumes of water. Schlieren optical pathways were employed using white spectrum point sources, as well as laser in the visible and near-infrared emission range (Strickler, 1977; Strickler and Hwang, 1999; Strickler and Balázsi, 2007). Doall *et al.* (1998) used the advantage of the long distance between the object and the image to split the original collimated laser beam in two beams crossing each other perpendicularly in the vessel of the animals. The subsequent combination of the two beams in one gave us a beam that carried the information of the front and side view of each phase object swimming around in the vessel. The result was then a dark-field picture of the vessel with white to light grey images of the objects. A single video camera was used to register the events. The task to evaluate the videos in the late 20th century was to click on the object frame-by-frame, giving us the 3D coordinates at 60 Hz.

Figure 1 shows the time before a mating event as observed by Doall *et al.* (1998). The female starts at position a' and the male a little later at position a. The male meets the track of the female at position b, takes a turn and follows the track of the female. However, the male follows the track in the wrong direction. After 1.2 s it turns and back-tracks to catch up with the female at position c. In 27 of 67 pursuit observations (40 %) the male started in the wrong direction, which does not suggest a good method to determine the direction at the moment of finding the trail. In 22 out of 27 observations when the initial swimming direction was incorrect the male turned around (81 %). Thus, in a total of 92 % of cases, the male eventually followed the female in the correct direction, a remarkable achievement for any member of the animal kingdom. Back tracking with similar time components was also observed in presence of trails simulating tracks from swimming zooplankters (Yen *et al.*, 2004).

3. The Spiking Neuron Model for Ratio Detection

Simple phenomenological spiking neuron models are very useful for investigation of neural coding, memory and other functions, as they are easier to analyze than detailed electrophysiological neuron models; see Gerstner *et al.* (2014) for a thorough introduction to both classes. The simplest form of the LIF model for a single neuron is given by the following differential equation for the membrane potential v

$$\tau \frac{dv}{dt} = -v(t) + RI(t), \tag{1}$$

where τ is the membrane time constant, R is the resistance of the membrane and I is an external current, if present. Spikes are generated whenever the membrane potential reaches a threshold ϑ. Then the membrane potential is reset to the resting potential v_r,

$$\text{if } v(t-) = \vartheta, \text{ then } v(t+) = v_r,$$

which also defines t as the spiking time of the LIF neuron. A schematic output of a LIF neuron with a single excitatory input is shown in Figure 2. For simplicity, a spike of the presynaptic neuron causes an immediate increase in the membrane potential.

In: Trends in Copepod Studies - Distribution, Biology and Ecology ISBN 0000000000
Editor: Marco Uttieri, pp. 5-14

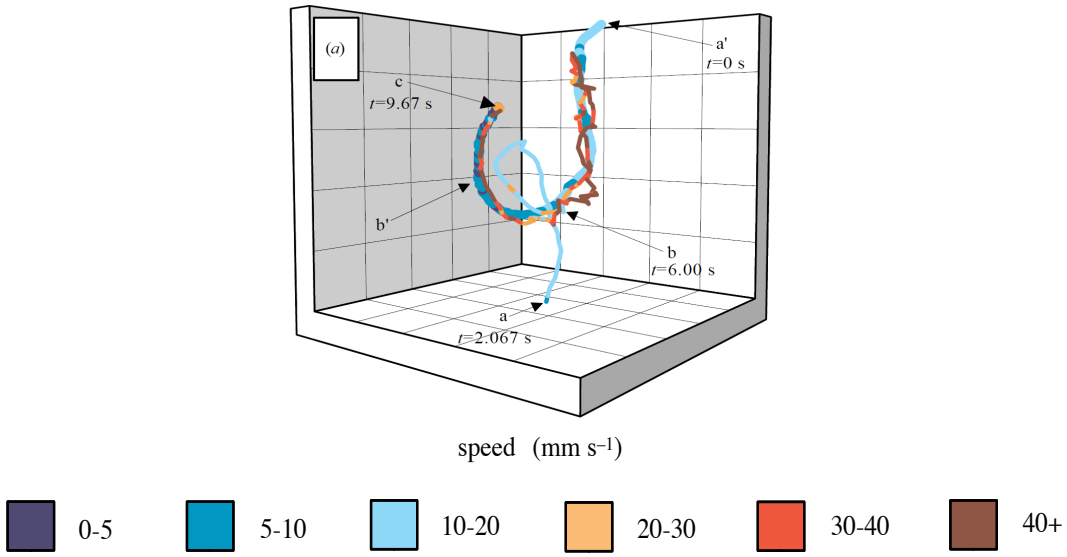

Figure 1. Trails of a female and a male from Doall *et al.* (1998). The fat and thin trails are that of the female and the male, respectively, while colors indicate swimming speeds. The male encounters the female's trail at position *b* and proceeds for the next ≈1.2 s in the wrong direction before turning around and finally capturing the female at position *c*. The grid unit is 1 cm. Reprinted from (Doall *et al.*, 1998) with permission from the Royal Society.

To model the synaptic connections between neurons we use the conductance-based model as described by Vogels and Abbott (2005). The sub-threshold membrane potential V and the excitatory, respectively inhibitory conductances g_{ex} and g_{inh} are governed by

$$\tau \frac{dV}{dt} = (V_r - V) + g_{ex}(E_{ex} - V) + g_{inh}(E_{inh} - V), \tag{2}$$

$$\tau_{ex} \frac{dg_{ex}}{dt} = -g_{ex}, \tag{3}$$

$$\tau_{inh} \frac{dg_{inh}}{dt} = -g_{inh}, \tag{4}$$

as long as no spiking takes place. We choose the resting potential $V_r = -60$ mV, the relaxation time constant for the membrane $\tau = 20$ ms and the synaptic time constants $\tau_{ex} = 5$ ms and $\tau_{inh} = 10$ ms, respectively (Vogels and Abbott, 2005). The key difference in the influence of the excitatory and inhibitory conductances is that the two reversal potentials are chosen to be $E_{ex} = 0$ mV and $E_{inh} = -80$ mV, respectively. Once the membrane potential reaches the threshold of $\vartheta = -50$ mV, the time is recorded as a spiking time and V is reset to V_r. Upon spiking of a presynaptic neuron at time t, all postsynaptic neurons have their excitatory respectively inhibitory conductances changed by a certain amount, depending on the nature of the synapse. If the synapse is excitatory, the excitatory conductance of the postsynaptic neuron is increased,

$$g_{ex}(t+) = g_{ex}(t-) + w_{ex}, \tag{5}$$

In: Trends in Copepod Studies - Distribution, Biology and Ecology ISBN 0000000000
Editor: Marco Uttieri, pp. 6-14

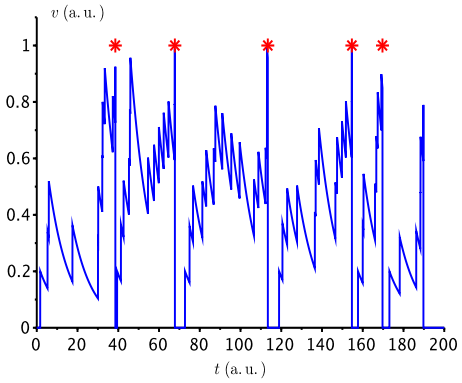

Figure 2. The membrane potential v of a LIF neuron governed by Equation (1) with $I \equiv 0$ that receives a single excitatory input ("a.u." = auxiliary unit). At each incoming spike, v is increased by 0.2. The spiking times of the neuron are indicated by red dots.

if the synapse is inhibitory, the inhibitory conductance of the postsynaptic neuron is increased,

$$g_{inh}(t+) = g_{inh}(t-) + w_{inh}. \tag{6}$$

The amounts of increase in the respective conductances of the postsynaptic neuron are called the *weights* of the synapse. Their selection will be discussed in greater detail in Section 4. Note that these weights are non-negative in both cases and that only one of them characterizes a synapse.

A network topology for a ratio detection mechanism was proposed by Zavada *et al.* (2011). ORNs of types a and b are excited upon binding of their respective ligand. These are modeled as Poisson sources with firing rates r_a and r_b, respectively. Precisely, the probability that there are k spikes in a time interval Δt is

$$P\{k \text{ spikes during } \Delta t\} = \frac{e^{-r\Delta t}(r\Delta t)^k}{k!}.$$

Each ORN's firing rate grows linearly with respect to the logarithm of the ligand concentration u. This has been shown to hold for several orders of magnitude in the moth *Antheraea polyphemus* (Zack, 1979; Kaissling, 1996). For lack of better resources, we use the relationship

$$r = 48\lambda + 400,$$

where λ is the logarithm of the concentration of the compound, see Figure 3 in Kaissling (1996), ranging from -8 to -2, and r is the firing rate in Hz. This is the hypothetical response curve for both components of the mixture.

The ORNs are connected to two types of LNs by excitatory synapses. Each ORN of type a, respectively b, is connected to a specialist LN of the same type and these receive excitatory input only from the corresponding ORNs. Simultaneously, the ORNs also are connected to a generalist LN, that receives excitatory input from both types of ORNs. In both cases, there is a convergence ratio of N ORNs feeding a single LN. For simplicity, we

In: Trends in Copepod Studies - Distribution, Biology and Ecology ISBN 0000000000
Editor: Marco Uttieri, pp. 7-14

choose this convergence ratio to be the same for all excitatory connections. The LNs of all three types are connected by inhibitory synapses. We pick the smallest number possible, namely just one LN_a, one LN_b and one LN_{gen}. The synaptic connections are characterized by five weights where we make the following symmetry assumptions for the target ratio 1:1

1. the connections $\mathrm{ORN}_x \to \mathrm{LN}_x$ have the same weights for $x = a$ and $x = b$,
2. the connections $\mathrm{ORN}_x \to \mathrm{LN}_{gen}$ have the same weights for $x = a$ and $x = b$,
3. the mutual inhibition between LN_a and LN_b is symmetric,
4. $\mathrm{LN}_{a/b}$ act the same way on LN_{gen}, and
5. LN_{gen} acts the same way on $\mathrm{LN}_{a/b}$.

The network is depicted schematically in Figure 3. The output of the network is the firing rate of LN_{gen}. Note that by Dale's principle this output is necessarily inhibitory, as LN_{gen} already inhibits LN_a and LN_b. This signal is processed by further local intermediate neurons and projection neurons that we do not include in our model.

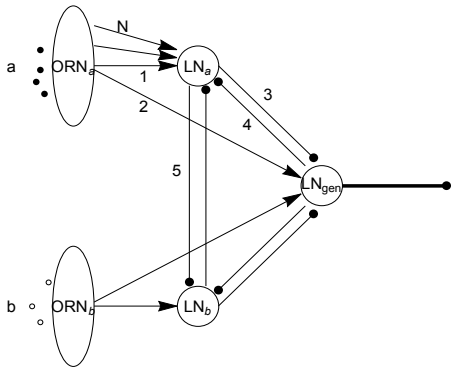

Figure 3. The topology of the ratio detection mechanism adapted from Zavada *et al.* (2011). Ligands of type "a" and "b" bind to the respective ORNs. The convergence from ORNs to LNs is indicated only once for clarity. Pointed and blunt arrows indicate excitatory respectively inhibitory relationships; labels indicate the independent weights.

The output of the generalist neuron LN_{gen}, *i.e.* its firing rate r_{gen} is the output of the mechanism, as a function of the firing rates r_a and r_b. If the mixture components a and b are present at the ratio $1:1$, both LN_a and LN_b inhibit each other. Thus the ORNs excite directly LN_{gen}. If, however, component a is present at a much higher concentration than component b, then LN_a will silence both LN_b and LN_{gen}, similarly if b is present at a much higher concentration than component a.

4. Synaptic Weight Selection

The spiking neuron model in Equations (2)-(6) is almost complete except for the choice of the synaptic weights. Recall that the weights are non-negative numbers associated with

each synapse. Thus the problem of choosing weights can be viewed as an optimization problem, where we optimize the network's behavior with respect to the desired output as a function of the five numerical weights. For each such weight vector we simulate the network behavior for selected ratios of $r_a : r_b$. Specifically, we use rates

$$r_a^i = r_0 \cdot 1.3^i, \quad r_b^j = r_0 \cdot 1.3^j, \tag{7}$$

for $i, j = 0, \ldots, 9$ and $r_0 = 10$ Hz. This corresponds to logarithmic concentrations ranging from 10^{-8} to 10^{-6}. While the ORN firing rates span a much larger range, we chose this range to demonstrate ratio detection at very low concentrations. The firing rate of LN_{gen} is recorded for each such simulation in a 10×10 response matrix $\mathbf{R}$. The numerical cost for each weight vector is defined to be the negative of the Frobenius inner product of the response matrix $\mathbf{R}$ with a convolution kernel $\mathbf{T}$ as in Figure 4,

$$C_{\mathbf{T}}(\mathbf{w}) = -\sum_{i,j=1}^{10} R_{i,j} T_{i,j}. \tag{8}$$

Note that for example negative off-diagonal entries in $\mathbf{T}$ strongly penalize against positive entries in the corresponding positions in $\mathbf{R}$.

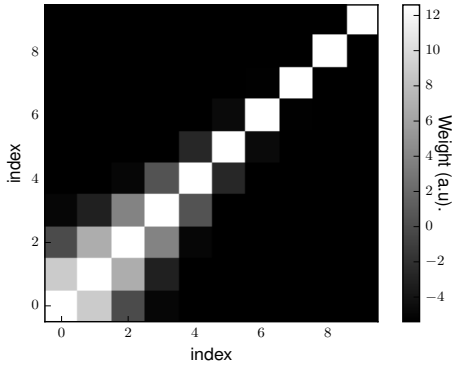

Figure 4. The convolution kernel $\mathbf{T}$ to determine the "cost" of the response matrix $\mathbf{R}$ used in Equation (8). The indices i and j are those from Equation (7).

We have implemented a SA algorithm (Press *et al.*, 2007, Section 10.12) to optimize the weights using the cost function in Equation (8). The PYTHON code is available from the github repository (Langhoff, 2017). The SA algorithm is built on an analogy from thermodynamics, namely the freezing and crystallization of liquids. Provided that the liquid cools sufficiently slowly, the constituents are able to align and to form ordered structures many orders of magnitude larger than the typical particle size. This amounts to a global minimization of the energy, as opposed to a rapid cooling that results only in a "quenched" or "amorphous" state corresponding to a local minimum. In practice, if a location $\mathbf{x}$ has been found, a random perturbation $\Delta\mathbf{x}$ is added. If $\Delta f = f(\mathbf{x}+\Delta\mathbf{x}) - f(\mathbf{x}) < 0$, then $\mathbf{x}+\Delta\mathbf{x}$ is chosen as the next point of the iteration. If $\Delta f = f(\mathbf{x}+\Delta\mathbf{x}) - f(\mathbf{x}) > 0$, then $\mathbf{x}+\Delta\mathbf{x}$ is chosen with a certain probability that is proportional to $\exp\left(-\frac{\Delta f}{T}\right)$, where T is the quantity analogous to temperature. Thus any improvement in the cost function is taken, while

In: Trends in Copepod Studies - Distribution, Biology and Ecology ISBN 0000000000
Editor: Marco Uttieri, pp. 9-14

a worsening is sometimes accepted, but less and less likely as the temperature decreases. The main choices to be specified are the generator for the random perturbations $\Delta\mathbf{x}$ and the method for decreasing T, called the "annealing schedule". Here we select $\Delta\mathbf{x}$ from a uniform distribution and enforce the constraint that all synaptic weights are non-negative. The temperature is multiplied by 0.85 every fifth iteration.

5. Results

We choose the convergence ratio of $N = 100$ ORNs feeding onto a single LN, for all possible ORN $\rightarrow$ LN connections. The optimal synapse weights are listed in Table 1.

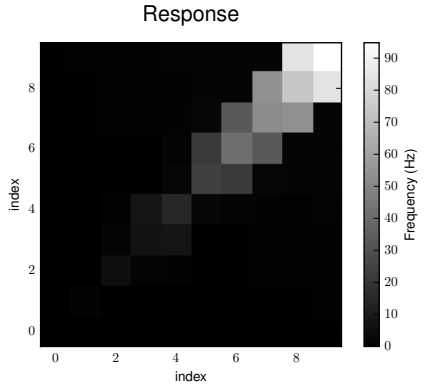

Figure 5. Optimal output of the network, defined as the LN_{gen} firing frequency. The (i, j)-entry corresponds to ORN firing frequencies of $10 \cdot 1.3^i$ Hz and $10 \cdot 1.3^j$ Hz respectively.

Connection	Weight (μS)
$\mathrm{ORN}_{a/b} \rightarrow \mathrm{LN}_{a/b}$	0.14025 (w_{ex})
$\mathrm{ORN}_{a/b} \rightarrow \mathrm{LN}_{gen}$	0.06980 (w_{ex})
$\mathrm{LN}_{a/b} \rightarrow \mathrm{LN}_{b/a}$	0.77945 (w_{inh})
$\mathrm{LN}_{a/b} \rightarrow \mathrm{LN}_{gen}$	0.64391 (w_{inh})
$\mathrm{LN}_{gen} \rightarrow \mathrm{LN}_{a/b}$	0.59438 (w_{inh})

Table 1. Optimal synaptic weights determined by the SA algorithm.

We note that the excitatory connections from the ORNs to the specialist LNs are stronger than to the generalist LN. Moreover, the mutual inhibition relations between the local neurons are roughly of similar strength. The model is somewhat limited in its discriminatory power at the lower end of the concentration ranges which may be caused by its strong simplification. In future work one may increase the number of LNs in the mutually inhibitory groups in the triangle in Figure 3 and include the subsequent intermediate LNs and projection neurons.

In: Trends in Copepod Studies - Distribution, Biology and Ecology ISBN 0000000000
Editor: Marco Uttieri, pp. 10-14

6. Conclusion

It is difficult for us humans to imagine how challenging pelagic copepod life must be. They live at low Reynolds number, at low population densities, and in the dark and three-dimensional ocean. With the adult males of some species even lacking functional mouth-parts, finding mates can absolutely not be left to chance. It is therefore natural for the males to respond to specific chemical signals (Yen and Lasley, 2011). To the best of our knowledge it is still an open question whether the copepod sex pheromones are specifically produced by the female or whether they are incidental byproducts of naturally occurring metabolism as, say, would be CO_2. Another important open question is how the well defined trails that were observed in water at rest are deformed and perhaps torn in the actual oceanic habitat of *Temora longicornis*.

We have shown that even a minimalistic, simplified neuronal model is capable of ratio detection. This represents a significant simplification from the previous model (Zavada *et al.*, 2011), where a full Hodgkins-Huxley model in addition to a rate-based Hodgkins-Huxley model of the neuron were used. Phenomenological models like the LIF model considered here do not explicitly model the individual ion channels in a neuron and treat spikes as formal events (Abbott, 1999). By omitting some of the biological details, we can gain insight into the behavior we seek to understand. The simplification is of course more relevant for much more complex networks, containing for example 10^5 neurons. In our case we see the relative weight of the neural pathways used for ratio detection. In reality, the ratio detection network will consist of more than just three LNs. At present little is known about the neuroanatomy of copepod brains and peripheral nervous systems, but there is evidence from the species *Tigriopus californicus* that it is endowed with a complex brain (Andrew *et al.*, 2011). In the future it will be valuable to investigate and to model the "spatial structure" that arises from the presence of ORNs on both antennas of the copepod sending signals to a pair of LN structures. We anticipate that further impulses for research will come from comparison with airborne arthropods due to the high level of conservation of neural circuitry in the pancrustaceans (the clade comprising crustaceans and hexapods).

So far only few semiochemicals used by copepods have been identified. One example is isophorone which is used by the parasitic sea louse *Lepeophtheirus salmonis* to locate its host, the Atlantic salmon *(Salmo salar)*, (Ingvarsdóttir *et al.*, 2002); see Figure 6. It has a molar mass of 138.21 g/mol and is used by airborne arthropods as semiochemical as well (El-Sayed, 2016). Very recently Selander *et al.* (2015) identified so-called "copepodamides" that signal to phytoplankton the presence of their zooplankton predators and thereby induce the production of toxins as a defense. Identification of such chemicals in seawater can be done by coupled liquid chromatography and mass spectrometry (LC-MS), and an electroantennographic detector (EAD) to confirm the response of the animal's antenna at precisely the moment that the chemical is detected. If there are candidates for the pheromone components, behavioral assays such as the Y-tube assay (Ingvarsdóttir *et al.*, 2002) can be used. Selander *et al.* (2016) present a list of 87 exudates from male and female *Temora longicornis*. Their list contains nine compounds that are produced mainly or even exclusively by the females. These compounds did not initiate the pursuit reaction in the male, but this can be because there were other volatile compounds that were not retained. Future research is needed to investigate the decay and diffusion rates of the com-

pounds and to locate potential differences. The number of compounds, their relatively large molecular masses (300-700 g/mol) and their likely complicated chemical structures indicate that a host of information should be available from their combined presence for the trained "observer".

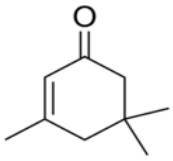

Figure 6. Isophorone is a kairomone used by the parasitic sea louse *Lepeophtheirus salmonis* to locate its host; (Ingvarsdóttir *et al.*, 2002). Structural formula from (Wikipedia, 2017).

All marine fauna are currently challenged by increasing chemical pollution and decreasing oceanic pH values, both of human origin. Changes in the background chemical landscape have harmful effects on olfactory-mediated behaviors in fish and crustaceans (Olsén, 2011). Due to their critical linking position in the marine food web, it is of high value to identify the chemical components of copepod sex pheromones and how their mating behavior is affected in the presence of pollutants.

Acknowledgements

We thank Dr. Marco Uttieri for the kind invitation to contribute to this volume. We thank him, Dr. Rachel Lasley-Rasher and Dr. Andrei Zavada for valuable comments that improved the manuscript considerably. PH acknowledges partial support from the Simons Foundation grant "Collaboration on Mathematical Biology" during a visit to the Georgia Institute of Technology. JRS's research was made possible by a grant from The Gulf of Mexico Research Initiative. Data are publicly available through the Gulf of Mexico Research Initiative Information & Data Cooperative (GRIIDC) at `https://data.gulfresearchinitiative.org`.

Abbreviations

LIF	Leaky Integrate-and-Fire.
LNs	Local Neurons.
ORNs	Olfactory Receptor Neurons.
SA	Simulated Annealing.

References

Abbott, L. F. 1999. "Lapicque's introduction of the integrate-and-fire model neuron (1907)." *Brain Research Bulletin* 50: 303–304.

Andrew, D. R., S. M. Brown, and N. J. Strausfeld. 2011. "The minute brain of the copepod *Tigriopus californicus* supports a complex ancestral ground pattern of the tetraconate cerebral nervous systems." *Journal of Comparative Neurology* 520: 3446–3470.

Bagøien, E., and T. Kiørboe. 2005. "Blind dating: mate finding in planktonic copepods. I. Tracking the pheromone trail of *Centropages typicus*." *Marine Ecology Progress Series* 300: 105–115.

Belmabrouk, H., T. Nowotny, J. P. Rospars, and D. Martinez. 2011. "Interaction of cellular and network mechanisms for efficient pheromone coding in moths." *Proceedings of the National Academy of Sciences USA* 108: 19790–19795.

Brunel, N., and M. C. W. van Rossum. 2007. "Lapicque's 1907 paper: from frogs to integrate-and-fire." *Biological Cybernetics* 97: 337–339.

Clifford, M. R. and J. A. Riffell. 2013. "Mixture and odorant processing in the olfactory systems of insects: a comparative perspective." *Journal of Comparative Physiology A* 199: 911–928.

deBruyne, M., and T. C. Baker. 2008. "Odor detection in insects: Volatile codes." *Journal of Chemical Ecology* 34: 882–897.

Doall, M. H., S. P. Colin, J. R. Strickler, and J. Yen. 1998. "Locating a mate in 3D: the case of *Temora longicornis*." *Philosophical Transactions of the Royal Society London B* 353: 681–689.

El-Sayed, A. M. 2003-2016. "The Pherobase: Database of Pheromones and Semiochemicals." `http://www.pherobase.com`; Accessed: March 2017.

Gadbois, S., and C. Reeve. 2014. "Canine olfaction: Scent, sign, and situation." In *Domestic Dog Cognition and Behavior*, edited by A. Horowitz, 3–29. Springer Verlag, Berlin, Heidelberg.

Gerstner, W., W. Kistler, R. Naud, and L. Paninski. 2014. Neuronal Dynamics. Cambridge University Press, Cambridge. Available at `http://neuronaldynamics.epfl.ch`. Accessed: March 2017.

Hepper, P. G., and D. L. Wells 2005. "How many footsteps do dogs need to determine the direction of an odour trail?" *Chemical Senses* 30: 291–298.

Hinow, P., J. R. Strickler, and J. Yen. 2017. "Olfaction in a viscous environment: The "color" of sexual smells in *Temora longicornis*." *The Science of Nature* 104: 46.

Hodgkin, A. L., and A. F. Huxley. 1952. "A quantitative description of membrane current and its application to conduction and excitation in nerve." *Journal of Physiology (London)* 117: 500–544.

Ingvarsdóttir, A., M. A. Birkett, I. Duce, R. L. Genna, W. Mordue, J. A. Pickett, L. J. Wadhams, and A. J. Mordue (Luntz). 2002. "Semiochemical strategies for sea louse control: host location cues." *Pest Management Science* 58: 537–545.

In: Trends in Copepod Studies - Distribution, Biology and Ecology ISBN 0000000000
Editor: Marco Uttieri, pp. 13-14

Kaissling, K. E. 1996. "Peripheral mechanisms of pheromone reception in moths." *Chemical Senses* 21: 257–268.

Katona, S. K. 1973. "Evidence for sex pheromones in planktonic copepods." *Limnology and Oceanography* 18: 574–583.

Langhoff, W. 2017. "Simulated Annealing Code for Ratio Detection." `https://github.com/WilliamLanghoff/ratio_detection`.

Lapicque, L. 1907. "Recherches quantitatives sur l'excitation électrique des nerfs traitée comme une polarization." *Journal de Physiologie et de Pathologie Générale* 9: 620–635.

Nihongi, A., S. B. Lovern, and J. R. Strickler. 2004. "Mate-searching behaviors in the freshwater calanoid copepod *Leptodiaptomus ashlandi*." *Journal of Marine Systems* 49: 65–74.

Olsén, H. K. 2011. "Effects of pollutants on olfactory mediated behaviors in fish and crustaceans." In *Chemical Communication in Crustaceans*, edited by T. Breithaupt. and M. Thiel, 507–529. Springer Verlag, New York, Dordrecht, Heidelberg, London.

Press, W. H., B. P. Flannery, S. A. Teukolsky, and W. T. Vetterling. 2007. Numerical Recipes: The Art of Scientific Computing. Cambridge University Press, Cambridge 3rd edition. Available at `http://apps.nrbook.com/empanel/index.html`. Accessed: March 2017.

Selander, E., J. Heuschele, G. M. Nylund, G. Pohnert, H. Pavia, O. Bjærke, L. A. Pender-Healy, P. Tiselius, and T. Kiørboe. 2016. "Solid phase extraction and metabolic profiling of exudates from living copepods." *PeerJ* 4: e1529.

Selander, E., J. Kubanek, M. Hamberg, M. X. Andersson, G. Cervin, and H. Pavia. 2015. "Predator lipids induce paralytic shellfish toxins in bloom-forming algae." *Proceedings of the National Academy of Sciences USA* 112: 6395–6400.

Settles, G. S. 2001. Schlieren and Shadowgraph Techniques. Springer Verlag, Berlin, Heidelberg, New York.

Seuront, L. 2013. "Chemical and hydromechanical components of mate-seeking behaviour in the calanoid copepod *Eurytemora affinis*." *Journal of Plankton Research* 35: 724–743.

Strickler, J. R. 1977. "Observing of swimming performances of planktonic copepods." *Limnology and Oceanography* 22: 165–170.

Strickler, J. R. 1998. "Observing free-swimming copepods mating." *Philosophical Transactions of the Royal Society London B* 353: 671–680.

Strickler, J. R., and G. Balázsi. 2007. "Planktonic copepods reacting selectively to hydrodynamic disturbances." *Philosophical Transactions of the Royal Society London B* 362: 1947–1958.

Strickler, J. R., and J.-S. Hwang, 1999. "Matching spatial filters in long working distance microscopy of phase objects." In *Focus on Multidimensional Microscopy*, edited by P. C. Cheng, P. P. Hwang, J. L. Wu, G. Wang, and H. Kim, 217–239. World Scientific, River Edge, NJ.

Töpler, A. J. I. 1866. "Ueber die Methode der Schlierenbeobachtung als mikroskopisches Hülfsmittel, nebst Bemerkungen zur Theorie der schiefen Beleuchtung." *Annalen der Physik* 203: 556–580.

Tsuda, A., and C. B. Miller. 1998. "Mate-finding behaviour in *Calanus marshallae* Frost." *Philosophical Transactions of the Royal Society London B* 353: 713–720.

Uttieri, M., A. Nihongi, M. G. Mazzocchi, J. R. Strickler, and E. Zambianchi. 2007. "Precopulatory swimming behaviour of *Leptodiaptomus ashlandi* (Copepoda: Calanoida): a fractal approach." *Journal of Plankton Research* 29: 17–26.

Vogels, T. P., and L. F. Abbott. 2005. "Signal propagation and logic gating in networks of integrate-and-fire neurons." *Journal of Neuroscience* 25: 10786–10795.

Weissburg, M. J., M. H. Doall, and J. Yen. 1998. "Following the invisible trail: kinematic analysis of mate-tracking in the copepod *Temora longicornis*." *Philosophical Transactions of the Royal Society London B* 353: 701–712.

Wells, D. L., and P. G. Hepper. 2003. "Directional tracking in the domestic dog, *Canis familiaris*." *Applied Animal Behaviour Science* 84: 297–305.

Wikipedia 2017. "Isophorone" `https://en.wikipedia.org/wiki/Isophorone`. Accessed: March 2017.

Wyatt, T. D. 2010. "Pheromones and signature mixtures: defining species-wide signals and variable cues for identity in both invertebrates and vertebrates." *Journal of Comparative Physiology A* 196: 685–700.

Yen, J., and R. Lasley. 2011. "Chemical communication between copepods: Finding the mate in a fluid environment." In *Chemical Communication in Crustaceans*, edited by T. Breithaupt. and M. Thiel, 177–197. Springer Verlag, New York, Dordrecht, Heidelberg, London.

Yen, J., A. C. Prusak, M. Caun, M. Doall, J. Brown, and J. R. Strickler. 2004. "Signaling during mating in the pelagic copepod, *Temora longicornis*." In *Handbook of Scaling Methods in Aquatic Ecology: Measurement, Analysis, Simulation* , edited by L Seuront, and P. G. Strutton, 149–159. CRC Press, Boca Raton.

Zack, C. 1979. Sensory adaptation in the sex pheromone receptor cells of saturniid moths. PhD thesis Ludwig Maximilians University Munich.

Zavada, A., C. L. Buckley, D. Martinez, J. P. Rospars, and T. Nowotny. 2011. "Competition-based model of pheromone component ratio detection in the moth." *PLoS One* 6: e16308.